ESI for: Structural properties of geminal dicationic ionic liquid/water mixtures: a theoretical and experimental insight.

Alessandra Serva,[a] Valentina Migliorati,*[a] Andrea Lapi,[a,b] Giuliana Aquilanti,[c] Alessandro Arcovito[d] and Paola D'Angelo*[a]

[a] Dipartimento di Chimica, Università di Roma "La Sapienza", P.le A. Moro 5, 00185 Roma, Italy.

[b] Istituto CNR di Metodologie Chimiche-IMC, Sezione Meccanismi di Reazione c/o Dipartimento di Chimica, Università di Roma "La Sapienza", P.le A. Moro 5, 00185 Roma, Italy.

[c] Elettra-Sincrotrone Trieste S.C.p.A s.s. 14, km 163.5, I-34149 Basovizza, Trieste, Italy.

[d] Istituto di Biochimica e Biochimica Clinica, Università Cattolica del Sacro Cuore L.Go F. Vito 1, 00168 Roma, Italy.

* p.dangelo@uniroma1.it, valentina.migliorati@uniroma1.it

Online Supplementary Information

Molecular Dynamics details

Classical MD simulations of $[C_3(mim)_2]Br_2$/water mixtures with different molar ratio and 1:70 $[C_n(mim)_2]Br_2$/water mixtures with different alkyl-bridge chain length have been carried out at room temperature in the NVT ensemble, with the Nosé-Hoover thermostat[1,2] (the relaxation constant used is 0.5 ps). The force field used for $[C_n(mim)_2]Br_2$ DILs was taken from Lopes and Padua,[3,4] with a minor modification for the $[C_2(mim)_2]^{2+}$ and $[C_3(mim)_2]^{2+}$ dications. In particular, we modified the partial atomic charges of the alkyl-bridge chain in order to preserve the total charge +2 of the dication, and the atomic charge symmetry of the alkyl chain between the two imidazolium rings. For $[C_2(mim)_2]^{2+}$, we distributed the residual charge to the only two carbon atoms of the alkyl-bridge chain and to their corresponding hydrogen atoms ($+0.05e$ on each carbon atom and $+0.04e$ on each hydrogen atom). So we obtained a final partial charge of -0.12e and $+0.13e$ for the carbon and hydrogen atoms of the spacer, respectively. Conversely, for the $[C_3(mim)_2]^{2+}$ dication we adopted the modification introduced by Yeganegi et al.[5] The SPC/E[6] model was used for water molecules, since it provides a reliable description of the structural and dynamic properties of water.[7] All the Lennard-Jones parameters for different atom types have been calculated through the Lorentz-Berthelot combining rules, with the exception of the Br^--water interaction. In this case we adopted the OPLS force field,[8] for which we obtained the best agreement between the EXAFS experimental data and the theoretical signal of a $[C_3(mim)_2]Br_2$/water mixture with molar ratio of 1:70.

For all the simulations we used a timestep of 1 fs. The DIL and water molecules were positioned within a very large cubic simulation box in order to obtain the initial configurations, that was then compressed in the NPT ensemble at 1000 atm. The number of DIL and water molecules depends on the DIL/water molar ratio and computational cost. Then, the pressure was lowered to 1 atm and the systems were equilibrated in the NPT ensemble at 300 K for 1 ns to obtain the box edge length to be used in the production runs. A final equilibration NVT run was performed at 300 K for 3 ns, followed by a production run of 6 ns in which the configurations were saved every 200 timesteps. The intermolecular interactions were considered within a distance cutoff of 12 Å, while the Ewald summation method was adopted for electro-

static long-range effects.[9] The stretching interactions involving the hydrogen atoms were constrained through the SHAKE algorithm.[10] Additionally, a MD simulation of the Br^- ion in aqueous solution has been carried out, using a cubic box of one Br^- ion and 819 water molecules, and adopting the same MD protocol as that employed for the DIL/water mixture simulations. A homogeneous background charge was added to preserve the neutrality of the solution.

The radial and spatial distribution functions obtained from the MD trajectories have been used to describe the structural properties of the DIL/water mixtures under investigation. In particular, the radial distribution functions have been calculated using in-house written codes, while the TRAVIS software[11] was employed for the spatial distribution functions. The visualization software VMD[12] was used to provide the snapshots obtained from the MD simulations.

EXAFS sensitivity towards the dication atoms

From the MD results obtained in this work it is clear that the Br^- ions, besides interacting with the water molecules, are also well organised around the $[C_3(mim)_2]^{2+}$ dication in all the $[C_3(mim)_2]Br_2$/water solutions investigated by varying the water concentration (DIL/water molar ratios of 1:16, 1:28, 1:40, 1:70, 1:200 and 1:400). To understand why the dication atoms provide a negligible contribution to the EXAFS spectra we can compare the structural properties of the $[C_3(mim)_2]Br_2$/water mixtures studied here with those of imidazolium bromide ILs where the EXAFS theoretical signals associated with the imidazolium cation have been found to be non negligible.[13] In a recent MD-EXAFS study, the structural properties of pure alkylimidazolium bromide ILs, namely 1-alkyl-3-methylimidazolium bromide ($[C_n$mim]Br with n = 5, 6, 8, 10) have been studied, and the existence of a local order in these compounds has been evidenced, with the Br^- ions and imidazolium head groups forming a local three-dimensional bonding pattern that is common to all the $[C_n$mim]Br IL family, regardless of the length of the alkyl chain attached to the cation.[13] The Br K-edge XAS spectra were collected and they were reproduced by calculating the EXAFS theoretical spectra using the structural results obtained from MD simulations.[13] In these ILs, all the atoms of the cation imidazolium ring were found to contribute to the EXAFS theoretical signals, at variance with the results obtained here. To shed light on these differences, we have compared the $g(r)\rho$ functions be-

tween the bromide ions and the imidazolium ring atoms. In particular, we focused on the C and N atoms of the imidazolium ring that, having a higher scattering factor than the hydrogen atoms, are expected to provide a more significant contribution to the EXAFS signal. As a general trend, we found that, due to the presence of water molecules in the DIL/water mixtures, the cation-anion $g(r)\rho$'s shift towards larger distance values and the distribution becomes more unstructured as compared to pure monocationic ILs. As an example, Fig. S1 shows the comparison between the CR-Br $g(r)\rho$ calculated for pure $[C_6mim]Br$ and for the 1:16 $[C_3(mim)_2]Br_2$/water mixure. This solution has been chosen as, at this low water content, the amplitude of the $\chi(k)$ signals associated with the dication is expected to be larger. As it can be seen, the $g(r)\rho$ in the DIL/water mixture is shifted at higher distance values and becomes more disordered: the first shell peak positions are found at 3.72 and 3.63 Å and the coordination number calculated up to 4.5 Å is 1.0 and 1.5 for $[C_3(mim)_2]Br_2$/water mixure and pure $[C_6mim]Br$, respectively. Therefore, due to the presence of water molecules located between the Br^- ions and the imidazolium ring plane, the EXAFS signals associated with the imidazolium cation become less intense. Besides this, it is important to compare the overall intensity of the experimental EXAFS data, that in the $[C_3(mim)_2]Br_2$/water mixtures is about one order of magnitude larger as compared to pure $[C_nmim]Br$ ILs.[13] This is due to the presence of strong interactions between the Br^- ions and water molecules that give rise to a more intense EXAFS signal in which the low-amplitude contributions coming from the imidazolium cation are hardly detectable.

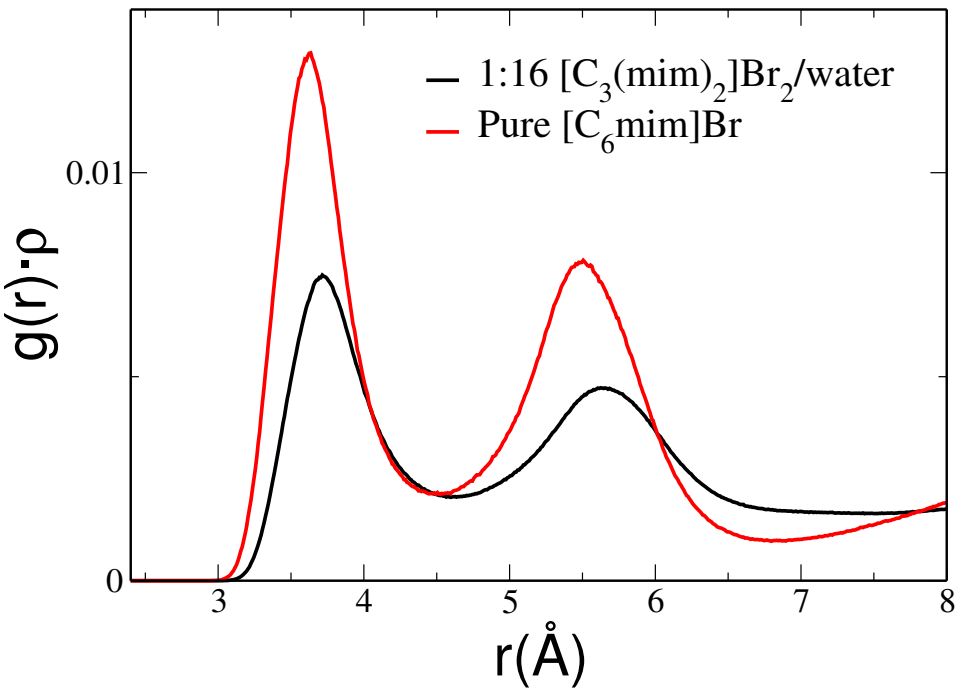

Figure S1. CR-Br radial distribution functions multiplied by the numerical densities, $g(r)\rho$, calculated from the MD simulations of the $[C_3(mim)_2]Br_2$/water mixture with molar ratio of 1:16 (black line) and of pure $[C_6mim]Br$ (red line).

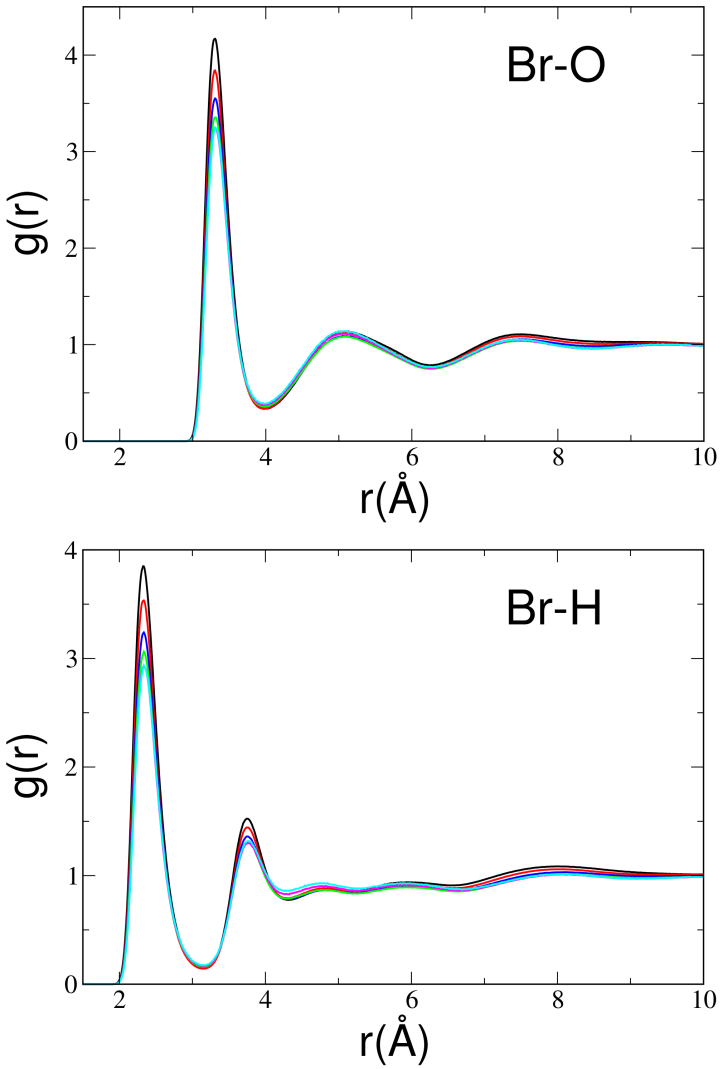

Figure S2. Radial distribution functions, $g(r)$'s, calculated from the MD simulations of the $[C_3(mim)_2]Br_2$/water mixtures with molar ratios of 1:16 (black line), 1:28 (red line), 1:40 (blue line), 1:70 (green line), 1:200 (magenta line) and 1:400 (cyan line). In the upper panel the Br-O $g(r)$'s are reported, while in the lower panel the Br-H $g(r)$'s. O and H are the oxygen and hydrogen atoms of the water molecules, respectively.

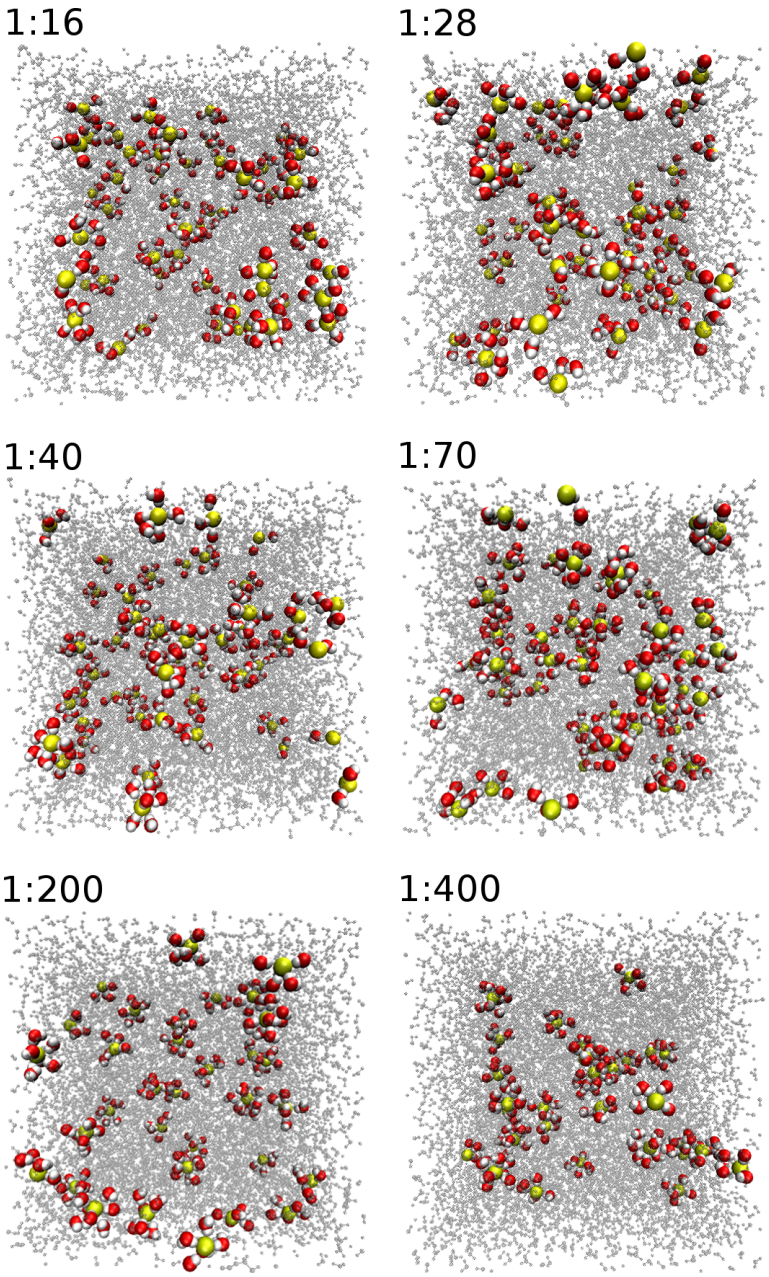

Figure S3. MD simulation snapshots of the $[C_3(mim)_2]Br_2$/water mixtures, showing the water molecules belonging to the bromide first hydration shell. The Br^- ion is colored yellow, while the oxygen and hydrogen atoms of the water molecules are red and white, respectively.

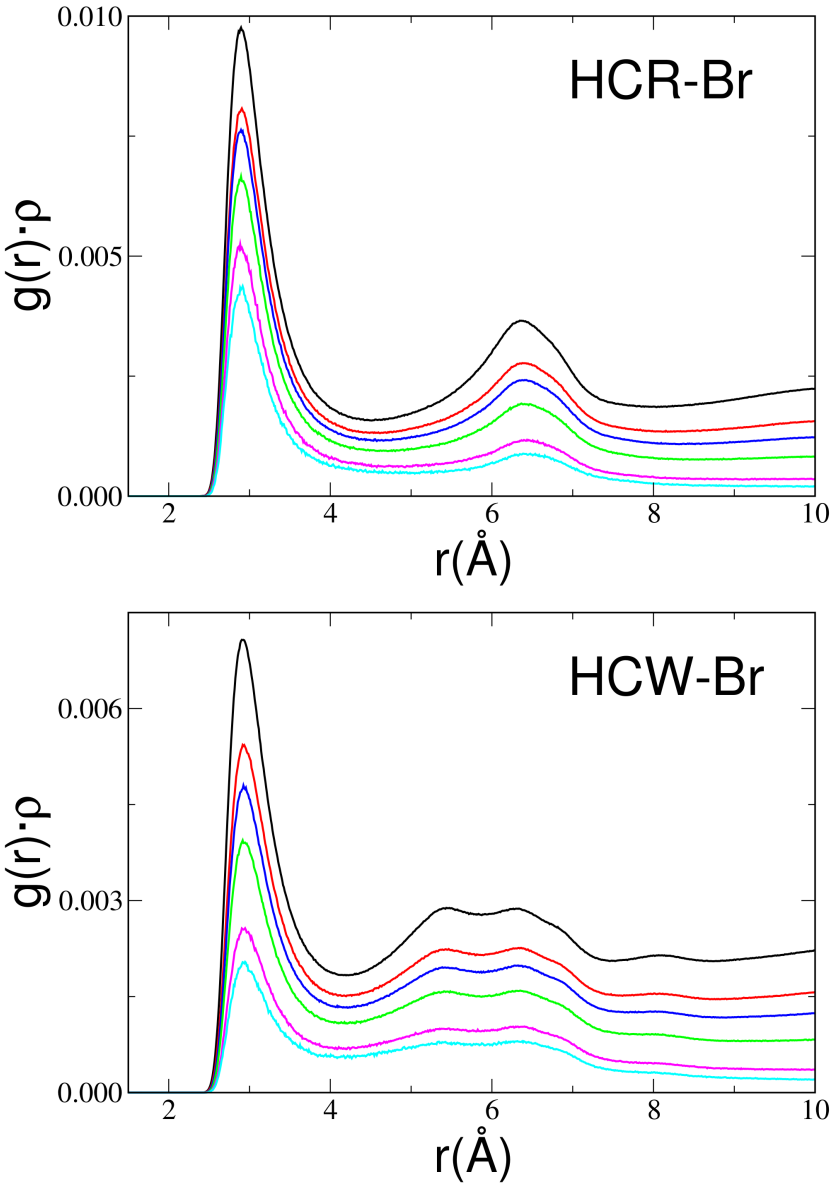

Figure S4. Radial distribution functions multiplied by the numerical densities, $g(r)\rho$, calculated from the MD simulations of the $[C_3(mim)_2]Br_2$/water mixtures with molar ratios of 1:16 (black line), 1:28 (red line), 1:40 (blue line), 1:70 (green line), 1:200 (magenta line) and 1:400 (cyan line). In the upper panel the HCR-Br $g(r)\rho$ functions are reported while in the lower panel the HCW-Br $g(r)\rho$'s.

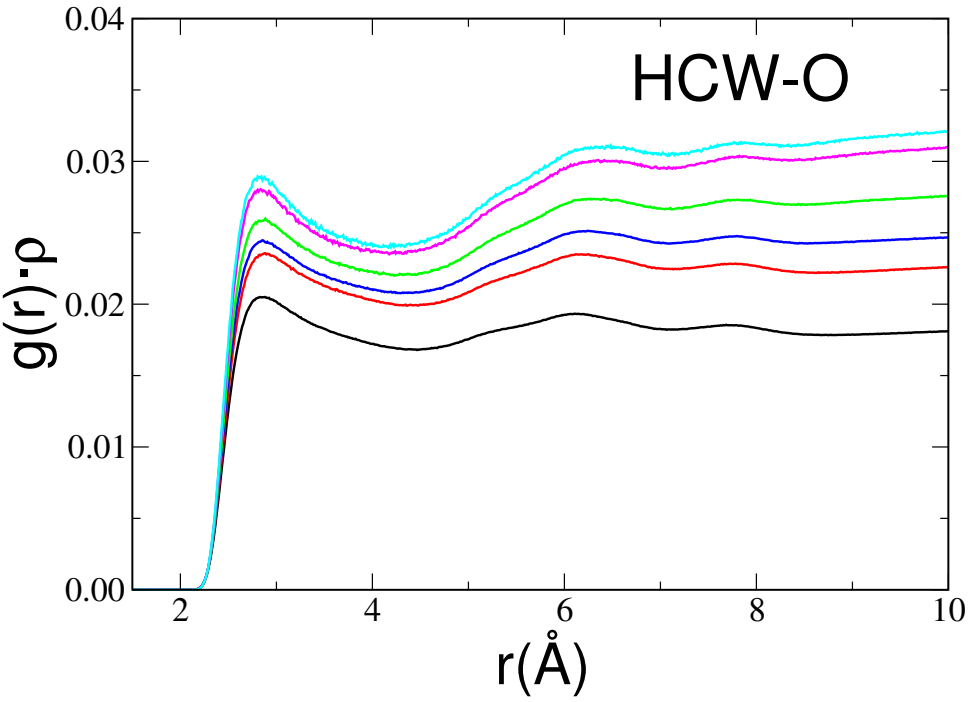

Figure S5. HCW-O radial distribution functions multiplied by the numerical densities, $g(r)\rho$, calculated from the MD simulations of the $[C_3(mim)_2]Br_2$/water mixtures with molar ratios of 1:16 (black line), 1:28 (red line), 1:40 (blue line), 1:70 (green line), 1:200 (magenta line) and 1:400 (cyan line). Note that O is the oxygen atom of water molecules.

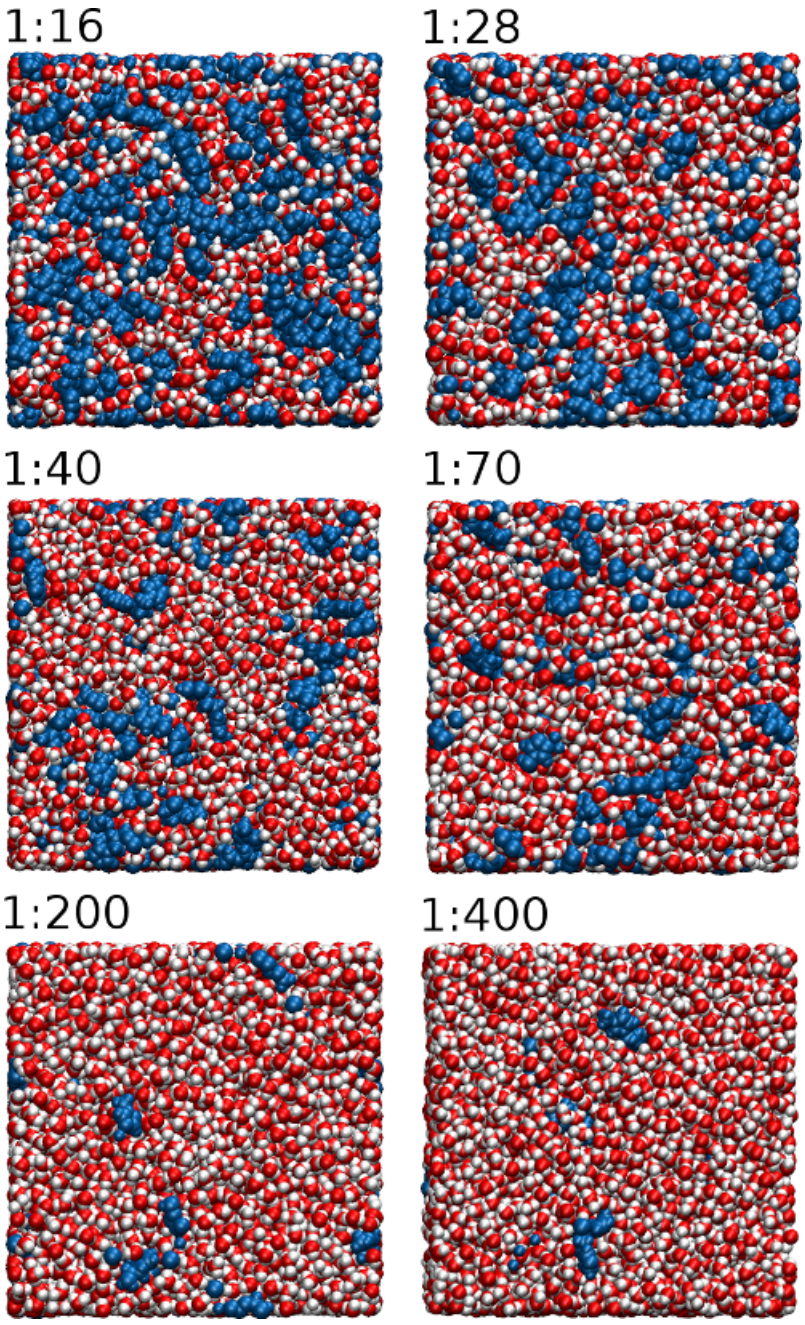

Figure S6. MD simulation snapshots of the $[C_3(mim)_2]Br_2$/water mixtures, where the water molecules are highlighted, while the DIL ion pairs are colored in blue.

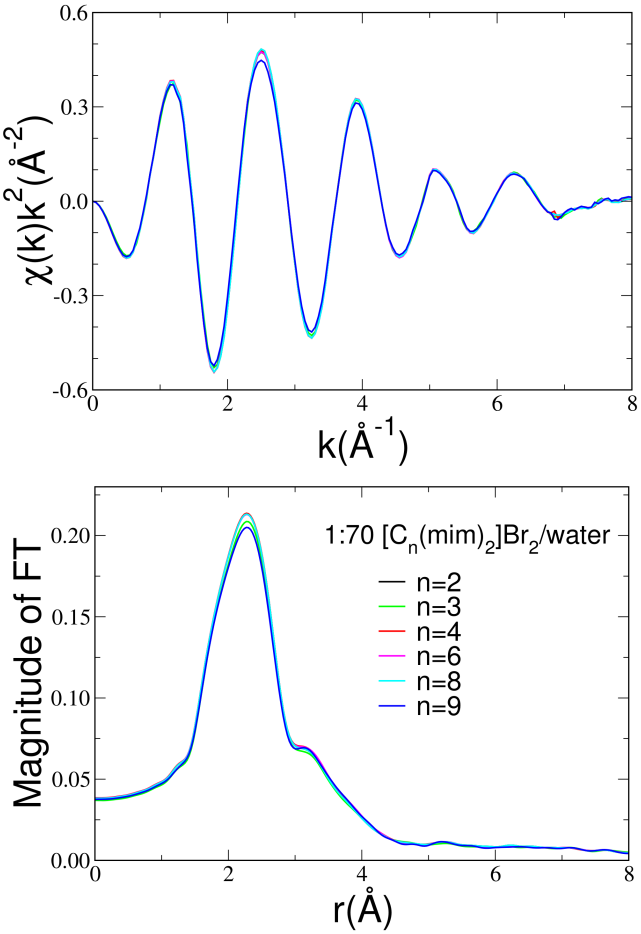

Figure S7. Upper panel: EXAFS experimental spectra of the 1:70 $[C_n(mim)_2]Br_2$/water mixtures with an alkyl-bridge chain length, n, of 2, 3, 4, 6, 8, 9. Lower panel: corresponding Fourier Transforms of the EXAFS experimental data.

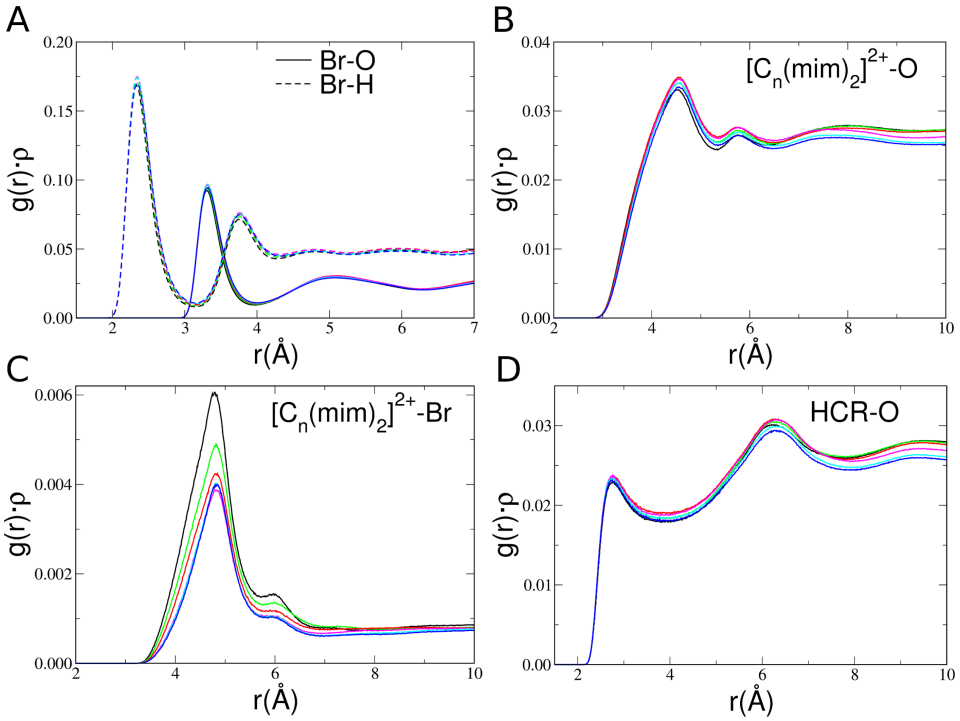

Figure S8. Radial distribution functions multiplied by the numerical density of the observed atoms, $g(r)\rho$, calculated from the MD simulations of the 1:70 $[C_n(mim)_2]Br_2$/water mixtures with an alkyl-bridge chain length, n, of 2 (black lines), 3 (green lines), 4 (red lines), 6 (magenta lines), 8 (cyan lines) and 9 (blue lines) carbon atoms. (A) Br-H (dashed lines) and Br-O (solid lines) $g(r)\rho$'s. (B) $g(r)\rho$'s calculated between one of the two ring geometrical centers of the $[C_n(mim)_2]^{2+}$ dication and the oxygen atom of water molecules, O. (C) $g(r)\rho$'s calculated between one of the two ring geometrical centers of the $[C_n(mim)_2]^{2+}$ dication and the Br^- ion. (D) $g(r)\rho$'s calculated between the most acidic hydrogen atom of the dication, HCR, and the oxygen atom of water molecules, O.

	R(Å)					
n	2	3	4	6	8	9
Br-O	3.33	3.33	3.33	3.33	3.33	3.33
$[C_n(mim)_2]^{2+}$-O	4.55	4.55	4.55	4.55	4.55	4.55
$[C_n(mim)_2]^{2+}$-Br	4.82	4.82	4.82	4.82	4.82	4.82
HCR-O	2.75	2.75	2.75	2.75	2.75	2.75
HCW-O	2.85	2.85	2.85	2.85	2.85	2.85
HCR-Br	2.90	2.90	2.90	2.90	2.90	2.90
HCW-Br	2.93	2.93	2.93	2.93	2.93	2.93

Table S1. Position of the $g(r)$ first peak, R, obtained from the MD $g(r)$'s of the 1:70 $[C_n(mim)_2]Br_2$/water mixtures with different alkyl-bridge chain length (n).

	N						cutoff (Å)
n	2	3	4	6	8	9	
Br-O	5.5	5.8	5.9	6.0	6.0	6.0	4.0
$[C_n(mim)_2]^{2+}$-O	13.1	13.4	13.7	13.6	13.3	13.2	5.3
$[C_n(mim)_2]^{2+}$-Br	1.9	1.6	1.4	1.2	1.2	1.2	5.8
HCR-O	5.2	5.3	5.5	5.4	5.3	5.3	4.3
HCW-O	6.2	6.3	6.4	6.3	6.2	6.1	4.3
HCR-Br	0.8	0.7	0.6	0.5	0.5	0.5	4.5
HCW-Br	0.6	0.5	0.5	0.4	0.4	0.4	4.5

Table S2. Coordination number, N, and cutoff distances obtained from the MD $g(r)$'s of the 1:70 $[C_n(mim)_2]Br_2$/water mixtures with different alkyl-bridge chain length (n). Note that the cutoff distances used in the calculation of N have been chosen as the position of the $g(r)$'s first minimum.

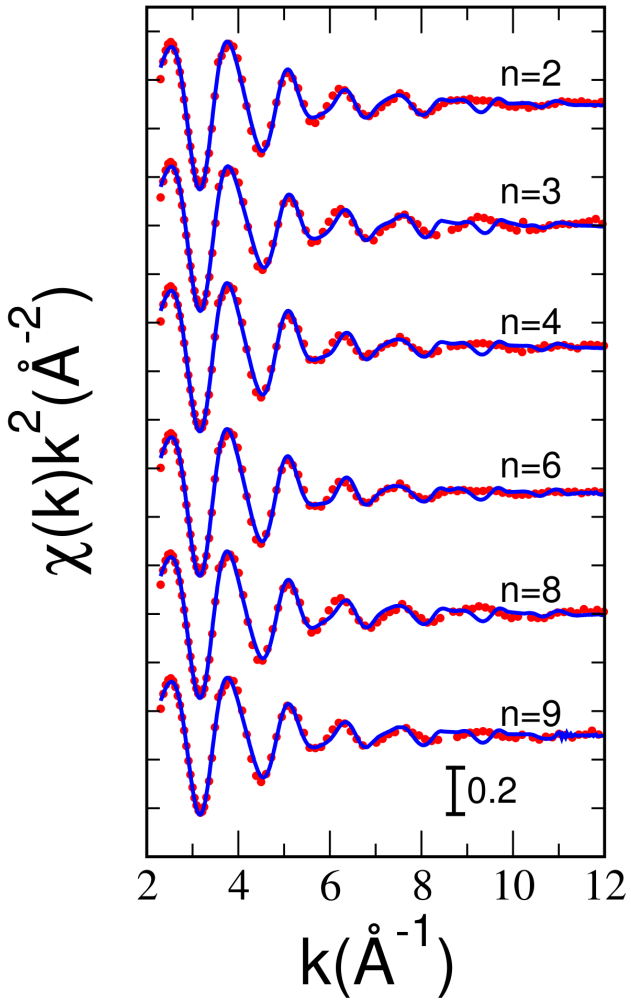

Figure S9. Comparison between the EXAFS experimental spectra (red dotted line) and the theoretical signals (solid blue line) calculated from the MD simulations of $[C_n(mim)_2]Br_2$/water mixtures with a constant DIL/water molar ratio of 1:70.

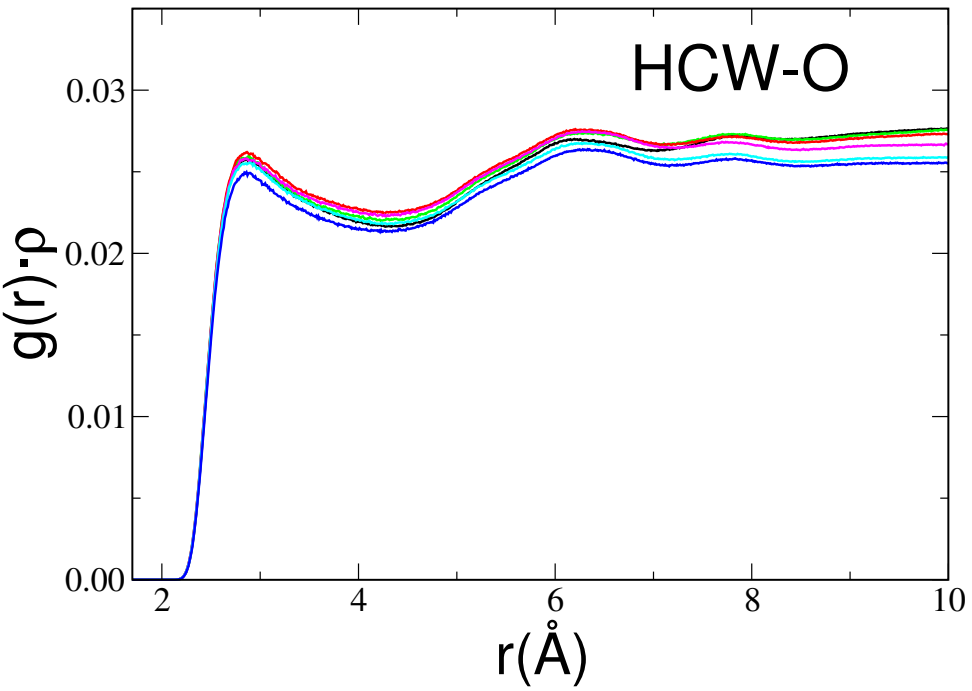

Figure S10. HCW-O radial distribution functions multiplied by the numerical densities, $g(r)\rho$, calculated from the MD simulations of the 1:70 $[C_n(mim)_2]Br_2$/water mixtures with an alkyl-bridge chain length, n, of 2 (black line), 3 (green line), 4 (red line), 6 (magenta line), 8 (cyan line) and 9 (blue line) carbon atoms. Note that O is the oxygen atom of water molecules.

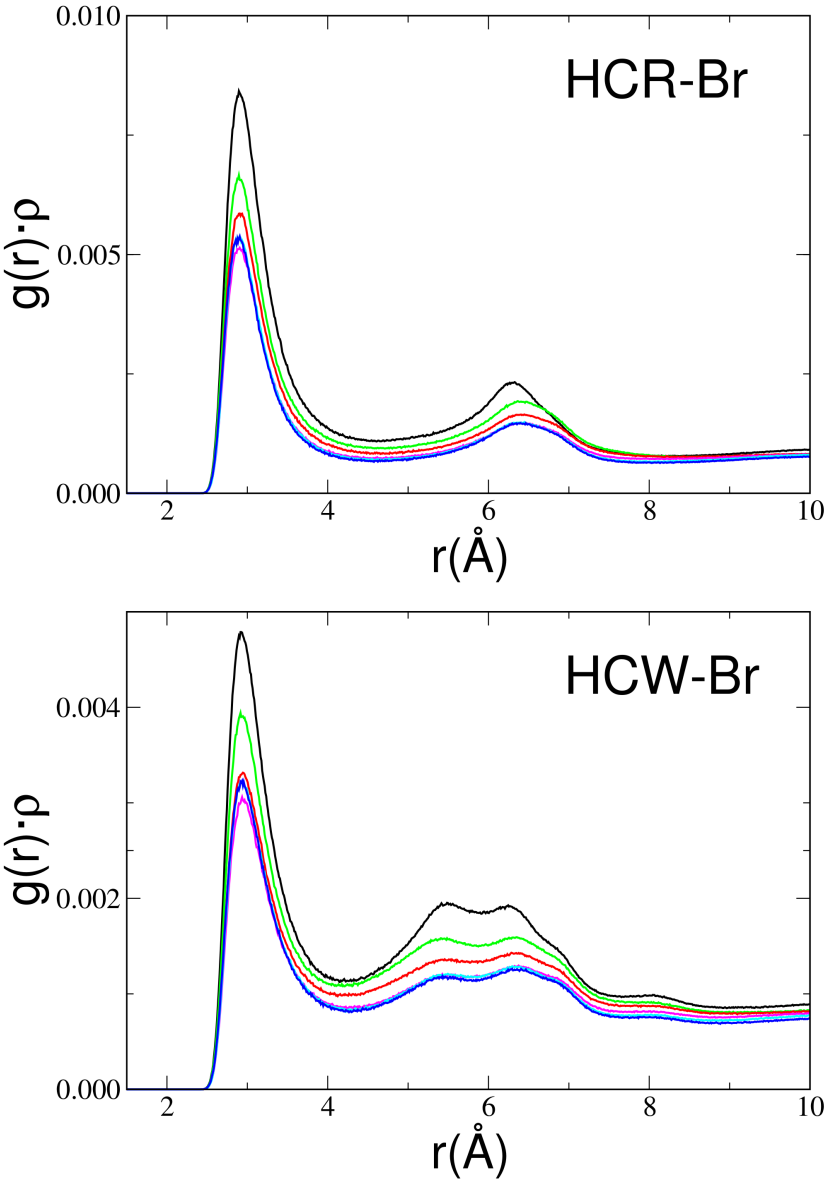

Figure S11. Radial distribution functions multiplied by the numerical densities, $g(r)\rho$, calculated from the MD simulations of the 1:70 $[C_n(mim)_2]Br_2$/water mixtures with an alkyl-bridge chain length, n, of 2 (black line), 3 (green line), 4 (red line), 6 (magenta line), 8 (cyan line) and 9 (blue line) carbon atoms. In the upper panel the HCR-Br $g(r)\rho$ functions are reported while in the lower panel the HCW-Br $g(r)\rho$'s.

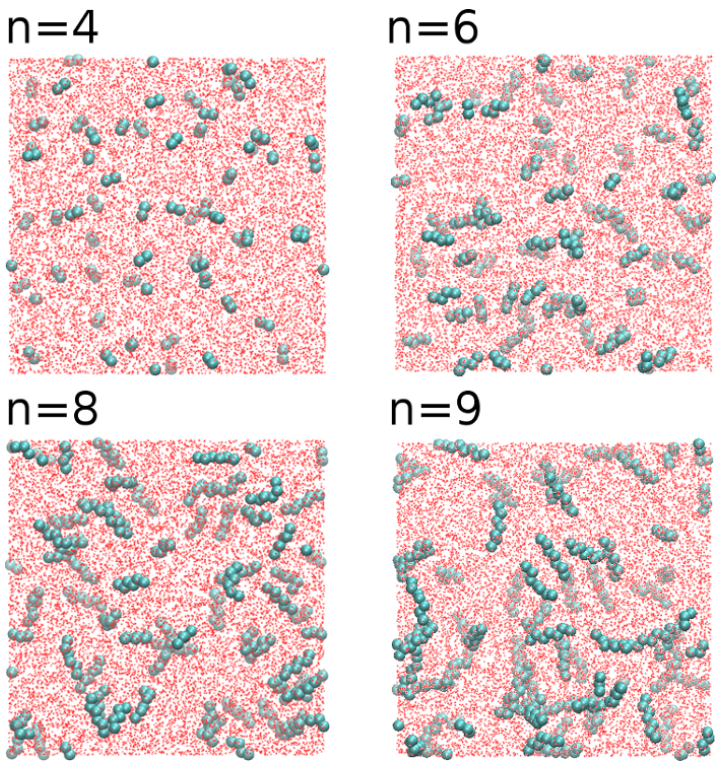

Figure S12. MD simulation snapshots of the $[C_n(mim)_2]Br_2$/water mixtures with n=4,6,8,9, where the alkyl-bridge chains are colored in cyan while all of the other atoms of the systems are represented as red dots.

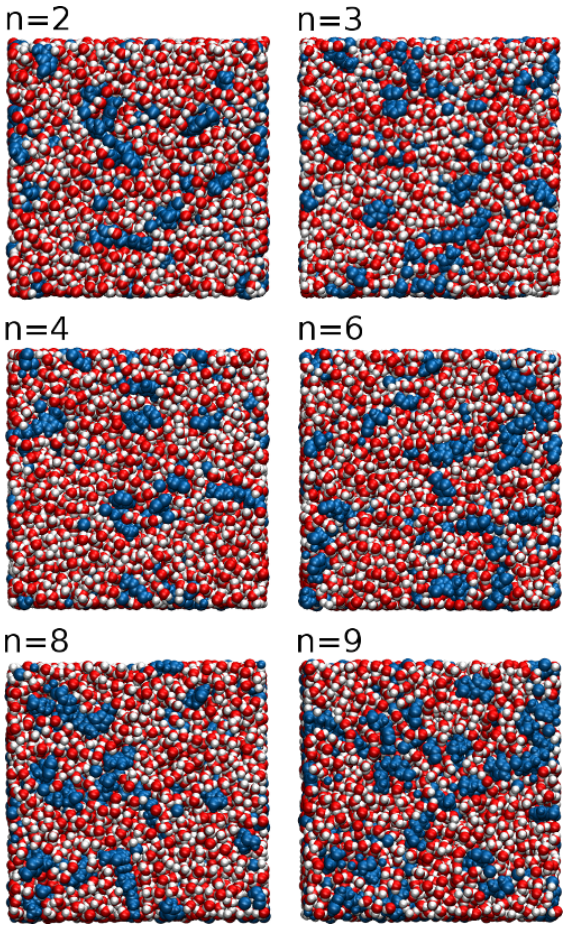

Figure S13. MD simulation snapshots of the 1:70 $[C_n(mim)_2]Br_2$/water mixtures with n=2,3,4,6,8,9, where the water molecules are highlighted, while the DIL ion pairs are colored in blue.

References

[1] S. Nosé, *J. Chem. Phys.*, 1984, **81**, 511–519.

[2] D. J. Evans and B. L. Holian, *J. Chem. Phys.*, 1985, **83**, 4069–4074.

[3] J. N. Canongia Lopes, J. Deschamps and A. A. H. Pádua, *J. Phys. Chem. B*, 2004, **108**, 2038–2047.

[4] J. N. Canongia Lopes and A. A. H. Pádua, *J. Phys. Chem. B*, 2006, **110**, 19586–19592.

[5] S. Yeganegi, A. Soltanabadi and D. Farmanzadeh, *J. Phys. Chem. B*, 2012, **116**, 11517–11526.

[6] H. J. C. Berendsen, J. R. Grigera and T. P. Straatsma, *J. Phys. Chem.*, 1987, **91**, 6269–6271.

[7] P. Mark and L. Nilsson, *J. Phys. Chem. A*, 2001, **105**, 9954–9960.

[8] W. L. Jorgensen, J. P. Ulmschneider and J. Tirado-Rives, *J. Phys. Chem. B*, 2004, **108**, 16264–16270.

[9] U. Essmann, L. Perera, M. L. Berkowitz, T. Darden, H. Lee and L. G. Pedersen, *J. Chem. Phys.*, 1995, **103**, 8577–8593.

[10] J.-P. Ryckaert, G. Ciccotti and H. J. Berendsen, *J. Comput. Phys.*, 1977, **23**, 327–341.

[11] M. Brehm and B. Kirchner, *J. Chem. Inf. Model.*, 2011, **51**, 2007–2023.

[12] W. Humphrey, A. Dalke and K. Schulten, *J. Mol. Graphics*, 1996, **14**, 33 – 38.

[13] V. Migliorati, A. Serva, G. Aquilanti, S. Pascarelli and P. D'Angelo, *Phys. Chem. Chem. Phys.*, 2015, **17**, 16443–16453.